

AD-A193 293

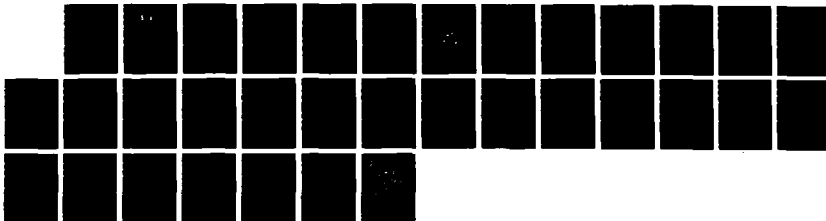
MIGRATION AND STABILITY OF HGCDE LATTICE DEFECTS(U)
WASHINGTON UNIV SEATTLE DEPT OF MATERIALS SCIENCE AND
ENGINEERING R KIKUCHI 29 FEB 88 ARO-23187. 3-PH
DAG29-85-K-0167

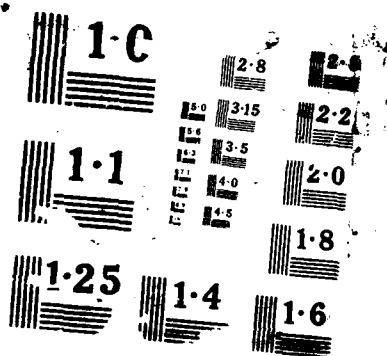
1/1

UNCLASSIFIED

F/G 20/2

NL





DTIC FILE COPY

(2)

AD-A193 293

UNCLASSIFIED
SECURITY CLASSIFICATION OF THIS PAGE

REPORT DOCUMENTATION PAGE

1a. REPORT SECURITY CLASSIFICATION Unclassified		1b. RESTRICTIVE MARKINGS	
2a. SECURITY CLASSIFICATION AUTHORITY DTIC SELECTED		3. DISTRIBUTION / AVAILABILITY OF REPORT Approved for public release; distribution unlimited.	
4a. DECLASSIFICATION / DOWNGRADING SCHEDULE APR 1 3 1988		5. MONITORING ORGANIZATION REPORT NUMBER(S) ARO 23187.3-PH	
6a. PERFORMING ORGANIZATION REPORT NUMBER(S) Co D		7a. NAME OF MONITORING ORGANIZATION U. S. Army Research Office	
8a. NAME OF PERFORMING ORGANIZATION University of Washington		9a. OFFICE SYMBOL (If applicable)	
9b. ADDRESS (City, State, and ZIP Code) Department of Mat. Sci. & Engr., FB-10 Seattle, WA 98195		10b. ADDRESS (City, State, and ZIP Code) P. O. Box 12211 Research Triangle Park, NC 27709-2211	
11a. NAME OF FUNDING / SPONSORING ORGANIZATION U. S. Army Research Office		11b. OFFICE SYMBOL (If applicable)	
12a. ADDRESS (City, State, and ZIP Code) P. O. Box 12211 Research Triangle Park, NC 27709-2211		13. PROCUREMENT INSTRUMENT IDENTIFICATION NUMBER DAAG29-85-K-0167	
14. SOURCE OF FUNDING NUMBERS PROGRAM ELEMENT NO. PROJECT NO. TASK NO. WORK UNIT ACCESSION NO.		15. TITLE (Include Security Classification) Migration and Stability of HgCdTe Lattice Defects	
16. PERSONAL AUTHOR(S) Ryoichi Kikuchi		17. TYPE OF REPORT Final Report	
18a. TIME COVERED FROM 6/24/85 TO 12/30/87		18b. DATE OF REPORT (Year, Month, Day) 88 February 29	
19. SUPPLEMENTARY NOTATION The view, opinions and/or findings contained in this report are those of the author(s) and should not be construed as an official Department of the Army position, policy, or decision, unless so designated by other documentation.		20. COSATI CODES FIELD GROUP SUB-GROUP	
21. SUBJECT TERMS (Continue on reverse if necessary and identify by block number)		22. ABSTRACT (Continue on reverse if necessary and identify by block number) Continuing from our previous work on equilibrium phase diagrams of Hg-Cd-Te systems, diffusion of Hg and Cd in HgCdTe has been studied in this project. The path probability method (PPM) of irreversible statistical mechanics is used with a point as the basic cluster. Basic formulation of diffusion A gradient of atomic density is applied to the system and the responding atomic flux is formulated. It is noteworthy to see that chemical potential gradient appears quite naturally as the driving force, as the Onsager theory requires, rather than the atomic density gradient. Hg fast diffusion It is made of two branches. In the vacancy mechanism branch, diffusion decreases with Hg vapor pressure, P(Hg), while it increases in the interstitial mechanism branch. Equations are derived to show these branches and curves for the diffusion coefficient are plotted. Experimentally observed activation energy is given atomic interpretation.	
23. DISTRIBUTION / AVAILABILITY OF ABSTRACT <input type="checkbox"/> UNCLASSIFIED/UNLIMITED <input type="checkbox"/> SAME AS RPT. <input type="checkbox"/> DTIC USERS		24. ABSTRACT SECURITY CLASSIFICATION Unclassified	
25a. NAME OF RESPONSIBLE INDIVIDUAL		25b. TELEPHONE (Include Area Code) 25c. OFFICE SYMBOL	

MIGRATION AND STABILITY OF HgCdTe LATTICE DEFECTS

Final Report

Ryoichi Kikuchi, Principal Investigator

February 29, 1988

U. S. ARMY RESEARCH OFFICE

DAAG29-85-K-0167 (U.W.)

DAAG29-84-K-0203 (UCLA)

**Department of Materials Science and Engineering, and
Advanced Materials Technology Program, Washington Technology Center
University of Washington
Seattle, WA 98195**

Approved for public release; distribution unlimited

Accession For	
NTIS CRA&I	<input checked="" type="checkbox"/>
DTIC TAB	<input type="checkbox"/>
Unannounced	<input type="checkbox"/>
Justification	
By	
Distribution	
Availability Codes	
Dist	Availability Codes
A-1	DTIC COPY INSPECTED 4

The view, opinions, and/or findings contained in this report are those of the author(s) and should not be construed as an official Department of the Army position, policy, or decision, unless so designated by other documentation.

1. Introduction

In the three year project preceding the present one, we theoretically studied the liquidus phase diagram of Hg-Te, Cd-Te, and then the ternary phase diagram of Hg-Cd-Te¹. All of these are equilibrium systems and the pair approximation of the cluster variation method (CVM)² was used for formulation. Based on this background, in the present three year project, we have studied time-dependent processes occurring in the $\text{Hg}_{0.8}\text{Cd}_{0.2}\text{Te}$ system. For this purpose we have used the path probability method (PPM)³ which is an extension of the CVM to time-dependent regime.

Examination of the HgCdTe lattice structure in Section 2 suggests the possible mechanisms of atomic migration: the vacancy mechanism, the interstitial mechanism, and a combination of the two. Based on these mechanisms, Section 3 develops the diffusion theory. Assuming that the Te diffusion is slow, the self diffusion coefficients of Hg and Cd are derived in terms of unit atomic jump probabilities.

The information thus obtained about atomic migration is then used in the theory of relaxation of the CdTe-HgCdTe junction. We summarize the relaxation theory in Section 4.

2. Structure of HgCdTe lattice

The HgCdTe crystal has the zincblende structure as shown in Fig. 1. It is made of two fcc sublattices, to be called I and II, as marked by white and black spheres. The Hg and Cd preferentially occupy I, and Te preferentially II. The centers of the cube edges in Fig. 1 will be called III. This is surrounded by six neighboring I sites and hence is an octahedral interstitial site of the I fcc lattice. The corresponding octahedral interstitial sites of the II sublattice will be called IV. Note that a corner cube in Fig. 1 marked by broken lines contains four I and four III sites. The center of the I-and-III cube is alternatively a II or IV site. Inversely, the center of a II-and-IV cube is alternatively a I or III site. These four cubes are illustrated in Fig. 2. A III site is surrounded by four II sites tetrahedrally as is seen in Fig. 2(d), and thus can be interpreted as a tetrahedral interstitial site of the II fcc lattice, as well as an octahedral interstitial site of the I fcc sublattice, as was observed above.

We see in Fig. 2(c) and (d) that the nearest neighbor arrangement of a I site and a III site are the same (except the directional nature of the covalent bonding between atoms on I and II positions), and are different from the neighbor arrangement around a II or a IV site. Based on this observation, we reason that when Cd or Hg is excited to an interstitial site, it will be to a III site rather than to a IV, although both are interstitial sites.

In this project, we are concerned about the diffusion of Hg and Cd species. Therefore, in order to avoid the treatment becoming unduly complex, we disregard migration of Te atoms whose diffusion is known to be slower than Hg or Cd. Then we can summarize the problem as follows. Hg and Cd atoms are preferentially on the sublattice I, and some of them are excited to the interstitial positions on the sublattice III. They migrate on these two sublattices (I and III). These migrations occur within the simple cubic lattice formed by I and III sublattices, since the Te lattice, II, is not involved in our formulation. There are three migration schemes: I to I, III to III, and the exchange between I and III sites. Inside the s.c. lattice, the first two are second neighbor jumps while the I - III jumps are the first neighbor jumps.

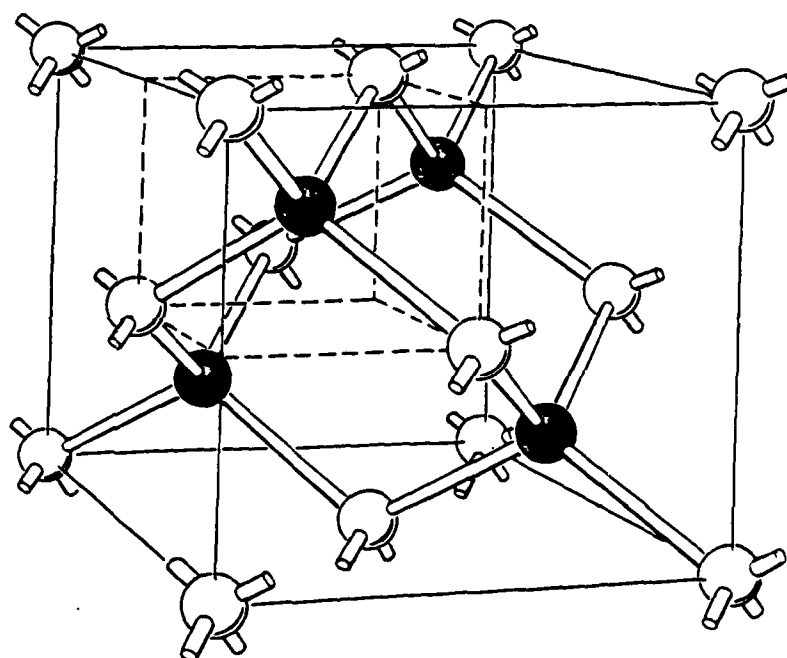


Figure 1(a). The zincblende structure of the Hg-Cd-Te crystal. It is made of two fcc sublattices, I (white sphere) and II (black sphere).

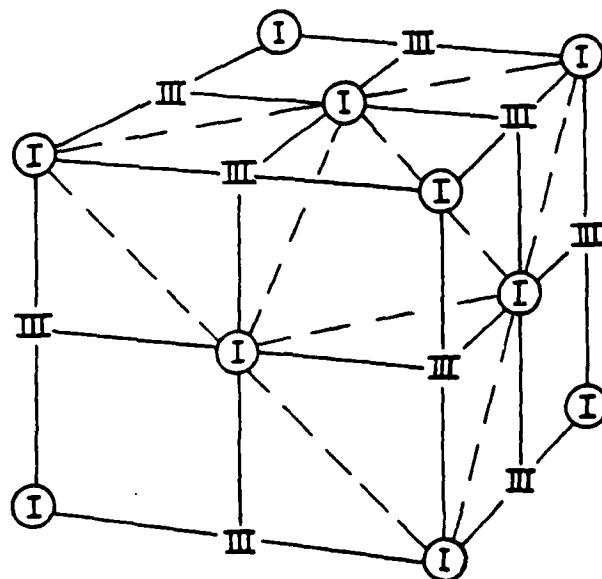
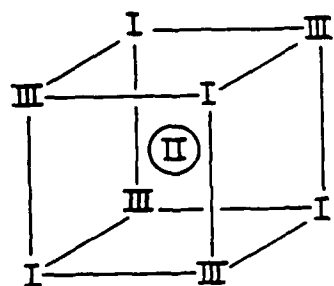
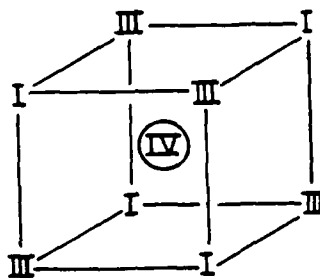


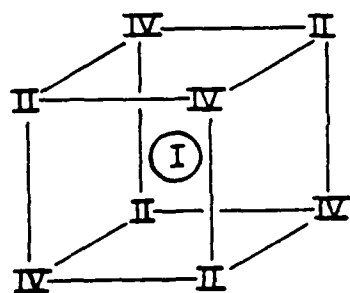
Figure 1(b). Geometry of the I sublattice and the interstitial III sites.



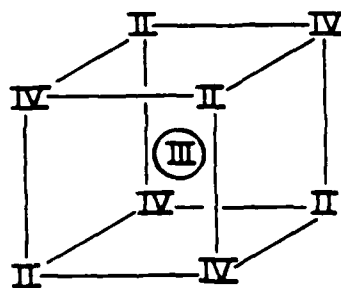
(a)



(b)



(c)



(d)

Figure 2. Relations between two main sublattices (I and III), and two interstitial sublattices (III and IV)

3. Diffusion of Hg and Cd

3.1 *Basics of the diffusion theory*

Diffusion of Hg and Cd is formulated using the path probability method (PPM)³ for irreversible statistical mechanics, which is an extension of the cluster variation method (CVM)² in equilibrium statistical mechanics. The CVM is known as the most efficient formulation for cooperative phenomena in crystalline systems. Applications of it to calculations of phase diagrams of solid state phases have been increasing to include complex phases and complex effects. The PPM is the time-dependent version of the CVM, and has been successful in deriving diffusion, and phase transition kinetics including nucleation kinetics.

The basic concept of the PPM is that change of state occurs in such a direction that the probability of change is a maximum. The basic mathematics of the formulation consists of three steps: (1) The first is to define variables which specify a state of the system, and also those which specify a direction of the change of a state in a short time interval. (2) The second is to formulate the probability of change in terms of these variables. This is an important step and is done using the entropy formulation of the CVM. (3) The third is to maximize the path probability function with respect to the variables, thus to find the most probable path, and then derive a set of differential equations to describe change of state.

3.2 *Choice of the basic cluster*

The first step in defining the basic variables to formulate the state and the diffusion is done by choosing the basic cluster. Since the formulation is done in the s.c. lattice involving the first and second neighbor pairs, the following alternatives are considered. (A) A choice which is satisfactory from the entropy point of view is to use a surface square of a s.c. unit cube. This choice is, however, mathematically complex at the present time, since it has four lattice points in the basic cluster. (B) The second acceptable choice is to use two basic clusters, the first neighbor pair and the second neighbor pair, simultaneously. (C) The third choice is to use a point as the basic cluster. This is not as satisfactory as the above two from the correlation point of view, but is mathematically the simplest and is considered sufficient to give qualitative information as an heuristic approach.

We made two formulations based on (B) and (C). The (B) formulation uses the first neighbor pair (I-III) and the second neighbor pairs (I-I and III-III) as the basic clusters. This formulation was the first time that two pairs were used in the PPM. However, the formulation took longer than expected, and thus it was decided to go to (C) before we come back to (B). Due to the time limitation, we could not finish (B), and the arrangement has been made that the unfinished work of (B) will be transferred to a project at Purdue University to complete. Diffusion formulation using a point as the basic cluster was also done by Ishikawa, Zhu and Sato recently⁴.

3.3 Equilibrium state for (C)

The first task which was finished and led to valuable information was (C). A paper is now being finished and will be published shortly. The formulation and the results are summarized here. Before going into the diffusion formulation, we review the equilibrium state and list key equations. As we discussed above, the system is made of two sublattices, I and III. On each lattice point one of the three species is found: a vacancy ($i=0$), a Cd atom ($i=1$) or a Hg atom ($i=2$). The probability of finding the i species on I is written as p_i and that on III as q_i . The interaction potential energy between i and j species is written as ϵ_{ij} for the first neighbor (I-III) pair, and as u_{ij} for the second-neighbor (I-I or III-III) pair. We assume that a vacancy does not contribute to a pair so that we require $\epsilon_{ij} = 0$ and $u_{ij} = 0$ when i or $j = 0$.

In order to estimate the energy constants, let us consider the CdTe system. In this case the sublattice I is preferentially occupied by Cd atoms and the sublattice III is almost vacant. We interpret this structure to mean that the I and III sublattices are in the ordered state of a binary system made of Cd atoms and vacancies. This can be realized when

$$\epsilon_{11} + \epsilon_{00} - 2\epsilon_{10} = \epsilon_{11} > 0.$$

On the other hand, the sublattice I does not split into further sublattices, so that we require

$$u_{11} + u_{00} - 2u_{10} = u_{11} < 0.$$

At this point we write the energy expression in the point approximation, which is also called the Bragg-Williams approximation or the mean field approximation. The nature of

the approximation is that the probability of finding a I-III pair, i on I and j on III, is approximated as $p_i q_j$, and the probability for an i - j pair on a I-I bond (on a III-III bond) as $p_i p_j$ (as $q_i q_j$). Since each I point has six III points in its nearest neighbors, and twelve I points in its second neighbors, the energy which an i atom on I feels, $E_i(p)$, and that on III feels, $E_i(q)$, are

$$E_i(p) \equiv \sum_{j=1}^2 (6\epsilon_{ij} q_j + 12u_{ij} p_j),$$

$$E_i(q) \equiv \sum_{j=1}^2 (6\epsilon_{ij} p_j + 12u_{ij} q_j).$$

When we write N for the number of points in a I sublattice, the energy for the system is written as

$$E = \frac{1}{2} [E_i(p) + E_i(q)].$$

The factor $1/2$ appears to avoid double counting of each pair. The entropy in the point approximation is written as

$$S = -kN(p_i \ln p_i + q_i \ln q_i).$$

When the free energy $E-TS$ is minimized with respect to p_i 's and q_i 's, we arrive at

$$p_i/p_0 = \exp[\beta\mu_i - \beta E_i(p)] > > 1,$$

$$q_i/q_0 = \exp[\beta\mu_i - \beta E_i(q)] < < 1,$$

where μ_i is the chemical potential of the i species ($\mu_0 = 0$). These relations are for $i=1$ and 2 , and the inequality signs are based on our requirement that vacancies on the I sublattice are few and the III sublattice is almost empty. We will use these relations in the discussions of diffusion in the following section.

3.4 Diffusion formulation based on (C)

The basic principle of the PPM, the time-dependent version of the CVM, is that the change of state occurs to such a direction that maximizes the probability of change (in a short time interval Δt), to be called the "path probability." This maximization process corresponds to the minimization of the free energy in the equilibrium theory.

In order to implement the maximization, we use the following steps: (1) We first define the "path variables" to describe change of state in Δt starting from a given state at t . These path variables are extension of the state variables p_i and q_i in Section 3.3. (2) Secondly the "path probability function" is written in terms of the path variables. The method of writing this function is the key of the PPM and uses the combinatorial formulation which is an extension of the CVM, taking into account the time axis as the additional dimension. (3) The next step is the maximization of the "path variable function" with respect to the path variables, keeping the state at t fixed: this leads to the most probable path within Δt . A set of differential equations to describe the change of system in time Δt can be derived. (4) Lastly to derive the differential equations, we apply chemical potential gradients $d(\beta\mu_i)/dn$ of the species 1 and 2 along the (111) direction of Fig. 1, and let atoms flow from one end of the system to the other. Figure 3 is a projection perpendicular to the (111) direction, and shows how lattice planes are numbered. We examine the stationary state in which the state variables do not change. The atom fluxes J_i are then proportional to the gradient $d(\beta\mu_i)/dn$, and the proportionality coefficient is the diffusion coefficient in the broad sense. (In the derivative, n indicates the position of the lattice plane.)

In this summary report, we do not go through the details of these four steps, but write the key results. The net flux toward the increasing n direction, $J_i^{(n)}$, at the n^{th} lattice plane is written in terms of jump probabilities, X 's, of i atoms (which are path probabilities) as

$$J_i^{(n)}(t)\Delta t = \frac{z}{2} [X_{0i,l}^{(n)}(t, t + \Delta t) - X_{i0,r}^{(n)}(t, t + \Delta t)],$$

where $X_{0i,l}^{(n)}$ is the probability of finding such lattice points (on the n^{th} plane) on which a vacancy at t is replaced by an i atom at $t + \Delta t$ which has come from the left.

Corresponding to the three migration schemes mentioned at the end of Section 2, the three components of J 's are $J_i(\text{I-I})$, $J_i(\text{III-III})$, and $J_i(\text{I-III})$. The most probable path condition mentioned in step (3) leads to

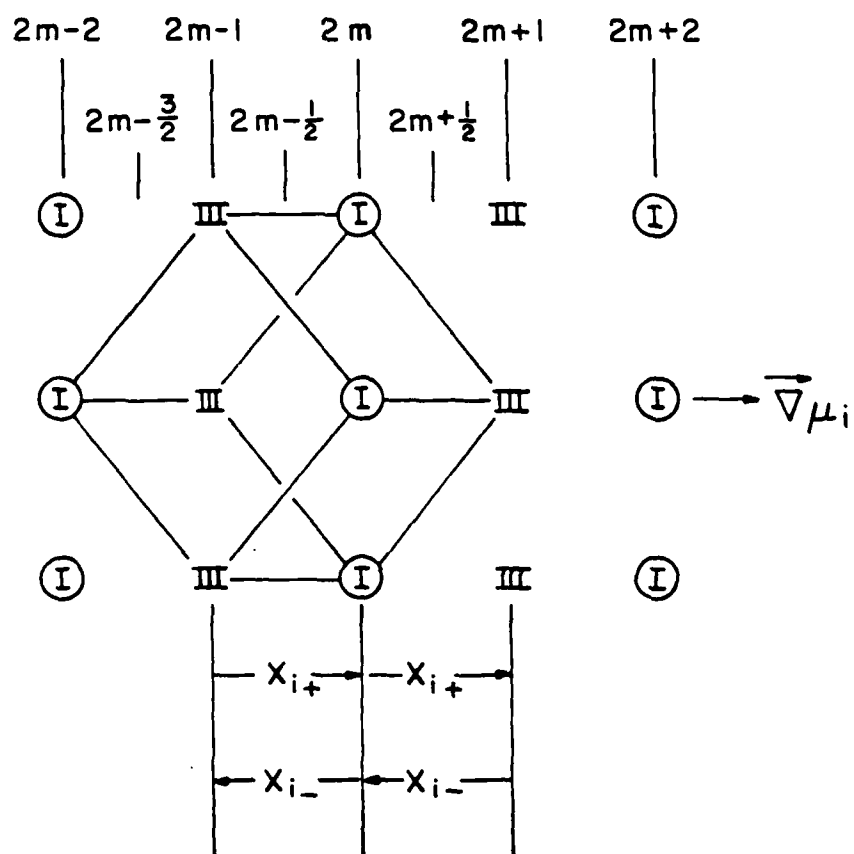


Figure 3. The [111] projection of I and III sublattices, and the direction of the chemical potential gradient.

$$J_i(I-I) = -\Theta(I-I) p_0 p_0 \frac{d}{dn} \exp(\beta \mu_i),$$

$$J_i(III-III) = -\Theta(III-III) q_0 q_0 \frac{d}{dn} \exp(\beta \mu_i),$$

$$J_i(I-III) = -\Theta(I-III) p_0 q_0 \frac{d}{dn} \exp(\beta \mu_i),$$

where Θ 's are the basic jump probabilities including the activation energies near the saddle points. It is gratifying from the point of view of irreversible thermodynamics that our fluxes are proportional to the gradient of $\beta \mu$'s, because the latter are the driving forces conjugate to atomic fluxes in the entropy production expression. We may also comment that when we write the flux relations in these forms, they are the same as those derived from a more accurate pair approximation (using a pair of lattice points as the basic cluster rather than a point in the present case). The difference in the point and the pair treatments lies in the chemical potential formulas.

In order to see the nature of the fluxes more explicitly, we need the μ expressions. In the point approximation of the present case, the equilibrium CVM leads to the p_i/p_0 and q_i/q_0 equations in Section 3.3. In these expressions, $E_i(p)$ and $E_i(q)$ are the energies per i species in I and III sublattices, respectively. We use these relations and rewrite J 's as

$$J_i(I-I) = -\Theta(I-I) p_i p_0 \exp[\beta E_i(p)] \frac{d(\beta \mu_i)}{dn}$$

$$J_i(III-III) = -\Theta(III-III) q_i q_0 \exp[\beta E_i(q)] \frac{d(\beta \mu_i)}{dn}$$

$$J_i(I-III) = -\Theta(I-III) p_i q_0 \exp[\beta E_i(p)] \frac{d(\beta \mu_i)}{dn}$$

where $E_i(p)$ [or $E_i(q)$] is defined in Section 3.3 and represents the energy of bonds to be broken when an i atom jumps away from a I [or III] site. To be more accurate, however, this energy estimate $E_i(p)$ should be modified with the term $-\sum u_{ij} p_j$ to eliminate the overcounting of the bond which does not exist because of the vacant site into which the atom is going to jump. Such overcounting is the nature of the PPM point approximation. Because of this inaccuracy

of overcounting, the point approximation has been usually avoided in the PPM. This inaccuracy is corrected in the pair approximation of the PPM which is now being formulated.

3.5 Comparison with experiments

Figures 4(a) through (d) show experimental results of J. Chen⁵ on Hg and Cd diffusion in HgCdTe by changing Hg vapor pressure, P_{Hg} . Note that D_{Hg} decreases with P_{Hg} in the low P_{Hg} region, and increases in the high P_{Hg} region. This behavior is understood from the last two equations.

The $J_1(I-I)$ flux is proportional to p_0 , the probability of vacancies in the I sublattice. In the low P_{Hg} region, a relatively large number of vacancies exist in the Hg-Cd (i.e. I) sublattice. As the Hg vapor pressure increases, most of the added Hg comes into the I lattice, resulting in less available vacancies, i.e. less p_0 , and hence in smaller value of $J_{Hg}(I-I)$. Thus we can interpret $J_2(I-I)$ as the vacancy mechanism of Hg diffusion occurring in the low P_{Hg} region.

In the high P_{Hg} region, the I sublattice is filled with Hg and Cd atoms, and hence as P_{Hg} increases Hg atoms go into the interstitial sublattice, III. The Hg flux $J_2(III-III)$ on III is proportional to the number of q_2 , the probability of Hg in interstitial positions, which increases with P_{Hg} . The probability of vacancies on the interstitial sublattice III is almost unity even when P_{Hg} increases. Thus we can interpret $J_2(III-III)$ as the interstitial mechanism of Hg diffusion which increases with P_{Hg} in the high P_{Hg} region. We thus identify $J_2(I-I) + J_2(III-III)$ as the fast component flux. The parameters used in this expression are then determined to fit experimental data. The resulting theoretical diffusion coefficient is then written as

$$D_{Hg} = 6 \times 10^{-14} \left[10^{13} p_0 \exp(-0.73eV/kT) + 10^8 q_{Hg} \exp(-0.18eV/kT) \right] \text{ cm}^2/\text{sec}.$$

Note that p_0 and q_{Hg} are theoretically calculated from the Hg vapor pressure P_{Hg} , which is uniquely determined by μ_{Hg} . When this is done the theoretical curve becomes as shown in Fig. 5. The interatomic energies and kinetic coefficients used in the computations are

$$-V_{Hg}(I-I) + E_{Hg}(p) = -0.73eV.$$

$$-V_{Hg}(III-III) + E_{Hg}(q) = -0.18eV.$$

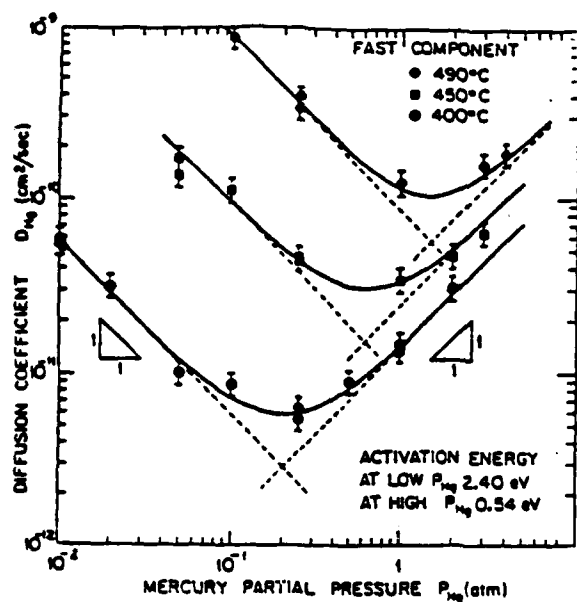


Figure 4a

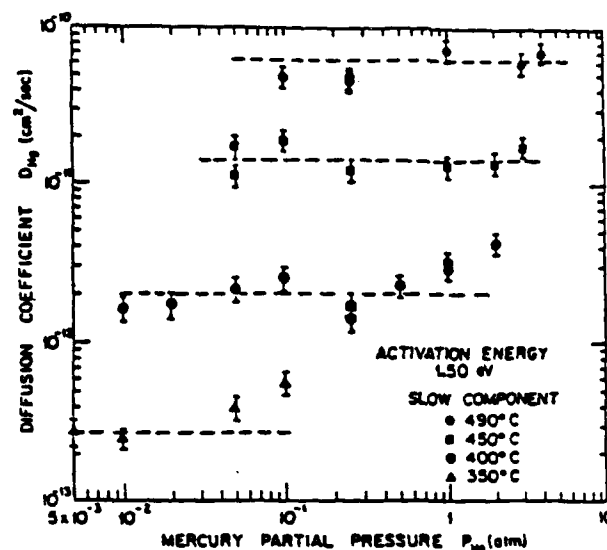


Figure 4b

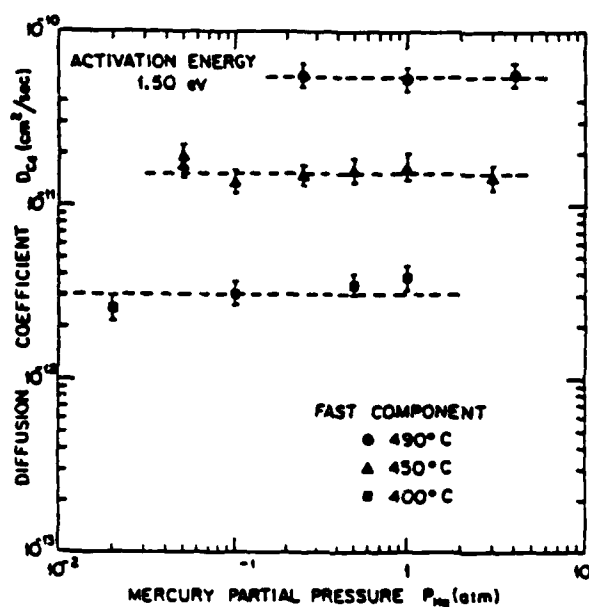


Figure 4c

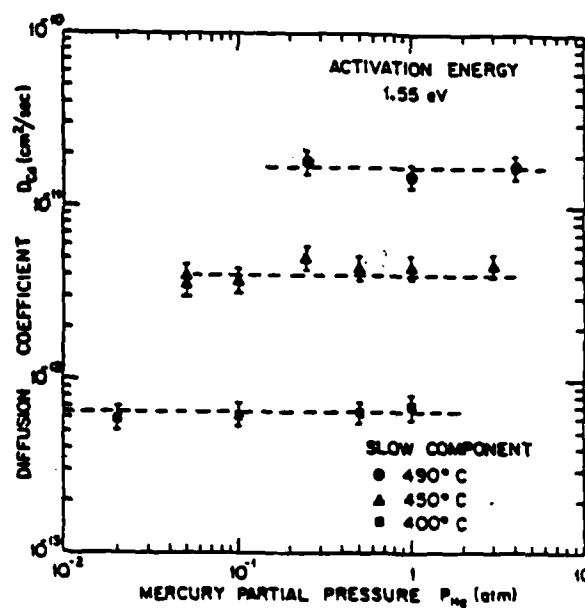


Figure 4d

Figure 4. (a) to (d) Experimental data of Hg and Cd diffusion after J. Chen.⁵

Diffusion Coeff. vs. Chem. Pot.

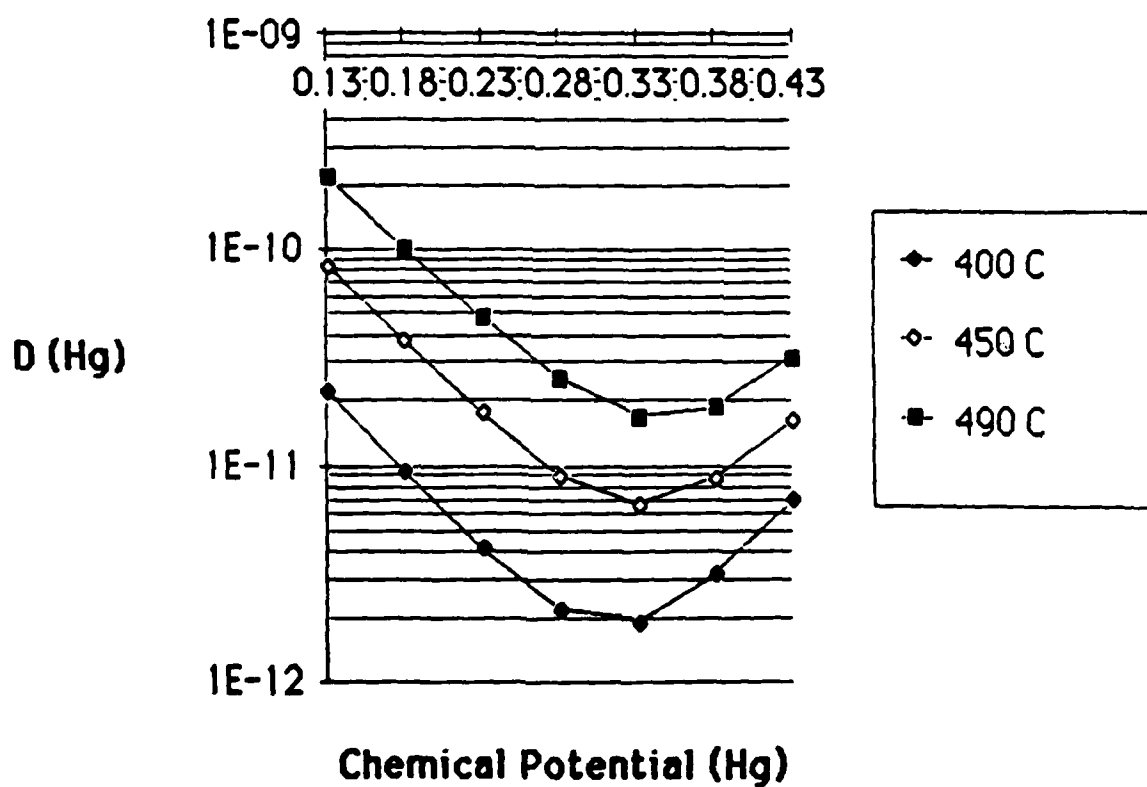


Figure 5. Theoretical Results of Hg diffusion (fast component) derived by the present work.

Where the E terms are the energies as defined in Section 3.3, and the V terms are the activation energies (excluding the bond-breaking energies) for atomic jumps in the I and III sublattices, respectively. We also identify the attempt frequencies (which are the vibrational frequencies) for the two sublattice positions as

$$\theta_{Hg}(I) = 10^{13} \quad \text{and} \quad \theta_{Hg}(III) = 10^8.$$

In the $J(I)$ expression we combined the θ factor and the V contribution as

$$\Theta_{Hg}(I - I) = \theta_{Hg}(I) \times \exp[-V_{Hg}(I - I)/kT].$$

It is understandable that the vibrational frequency on the interstitial position, $\theta(III)$, is much smaller than that for the substitutional I position, $\theta(I)$.

As is seen in Fig. 4(b), the slow diffusion component of Hg is independent of P_{Hg} . Different from Chen, we propose to identify it as the $I \rightarrow III$ and $I \leftarrow III$ jumps, because the $J_i(I-III)$ expression in Section 3.4 is proportional to $p_i q_0$ which is independent of P_{Hg} . Using the same value $\Theta_{Hg}(I) = 10^{13}$ of the fast component, the $J_i(I-III)$ expression leads to

$$D_{Hg,slow} = 0.3 \exp(-1.5eV/kT) \text{ cm}^2/\text{sec}.$$

The activation energy $1.5eV$ is taken from Chen's data. The preexponential factor 0.3 comes from our estimate of $\Theta_{Hg}(I) = 10^{13}$, and is acceptable compared with Chen's experimental value.

Chen's experiments show that Cd diffusion has the fast and slow components and both of them do not depend on P_{Hg} . Based on our interpretation, we identify Cd diffusion mechanism as the $I \rightarrow III \rightarrow I$ jumps. Using our $J_i(I-III)$ expression, and using Chen's estimate of the activation energy $1.5eV$, we can write

$$D_{Cd} = 0.3 \exp(-1.55eV/kT) \text{ cm}^2/\text{sec}.$$

Chen distinguishes the fast and slow components of Cd diffusion, although the difference is not very large. We cannot say definitely what is the cause of the two components, except a suggestion that neutral and charged Cd could be the reason.

4. Relaxation of CdTe-HgCdTe boundary

In semiconductor systems, the interest in layer structures is increasing explosively, both in basic studies and in practical applications, as evidenced by the proliferation of MBE machines. The present study is aimed at the question of the stability of the layer structure. We work on the CdTe-HgCdTe boundary and calculate how Hg diffuses into the CdTe crystal. The basis of the analysis is our knowledge of the migration kinetics of Hg and Cd atoms which was obtained by our diffusion studies summarized in Section 3.

We start with the same mathematical formulation as was used in the diffusion studies. The difference is that now we do not look at the stationary state, but work on the transient process to describe how the boundary changes in time.

When Hg atoms want to go into CdTe, since Hg diffusion via the interstitial mechanics is fast, it may seem that the boundary profile may change rapidly as Hg atoms diffuse. This argument does not hold, however, because Hg atoms in the interstitial sites in CdTe have to settle down to the substitutional Cd sites in order to complete the migration. This means Hg atoms have to wait for Cd atoms to be excited from their lattice sites and provide vacancies for Hg to drop into. Therefore, the excitation of Cd from I to III, which is slower than the interstitial Hg diffusion, is the rate controlling process.

The PPM formulation leads to the following set of differential equations to describe the change of Cd densities at each I lattice plane $2m$:

$$\frac{dp_I^{(2m)}}{dt} = 3 \left[J_{X_I}^{(2m-\frac{1}{2})} - J_{X_I}^{(2m+\frac{1}{2})} \right].$$

This set of differential equations for different values of m 's was to be solved numerically. Since the initial condition is that the boundary is sharp and the profiles of Cd and Hg atoms are step functions, we need to take special care in integration. We used the DGEAR subroutine in the IMSL library subroutine. Even with this subroutine, integration in the initial state was a difficult process.

In the above equation and in subsequent display of our results in Figs. 6 through 9, the lattice plane position is designated by m . The I lattice position is even, so that the index is $2m$. The III lattice is odd, and the index is $2m+1$. The position of an atomic jump is indicated

by the center of the bond on which the jump occurs. For example in the above equation, the first J term is from a III lattice plane $2m-1$ to a I plane at $2m$, so that this J is designated by $2m - \frac{1}{2}$.

As time proceeds, the profile rounds off. We calculated for three temperatures, 400°C, 500°C, and 550°C. Profiles for these temperatures for different times are shown in Fig. 6. The abscissa numbers, 1, 2, 3, etc., are the m values and indicate the position of the I sublattice. The three sets of curves in (a), (b), and (c) look similar, but the difference of the time scale is to be noted. The most gradual curves are for $t = 26$ sec, 2 sec, and 0.2 sec, respectively, for the three temperatures.

The three sets of curves in Fig. 7 plot the time evolution of $p_g^{(2m)}$ for different lattice positions. We observe that except in the very initial regions, the curves show trends of converging exponentially. Based on this behavior, we estimate relaxation times (τ 's) for each temperature at each m position. Figure 8 summarizes the results. From these plots, in turn, we can estimate activation energies for the diffusion process for lattice positions m . The values are plotted in Fig. 9. Since the junction region goes through drastic change, and may take long time to settle, we examine the activation energy for large $|m|$ regions. It is converging to 1.55 eV, the value for the Cd diffusion process, as we expected. This agreement shows the consistency of our calculation and the interpretation of the mutual diffusion.

Based on this study, we see that the relaxation time τ for the junction relaxation obeys the relation

$$\ln \tau = \frac{17333}{T} - 21.6,$$

where T is in Kelvin. Using this relation, the τ 's for low temperatures are 1.6 hrs, 40 days, and 2000 years for 300°C, 200°C and 100°C, respectively.

Fig 6(a). P(Cd) Profile at the Boundary
of Hg-Cd-Te/Cd-Te at 400 C.

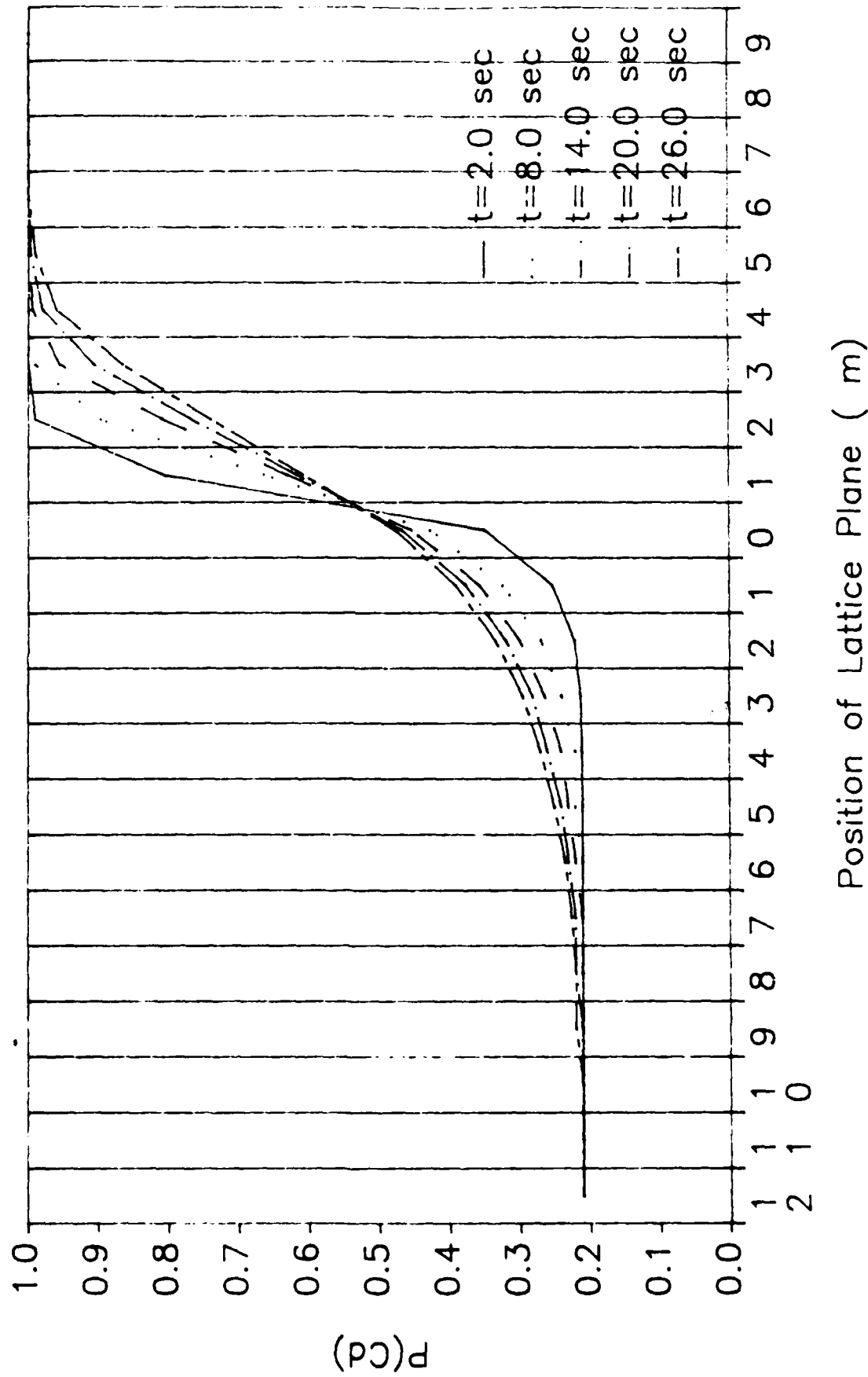
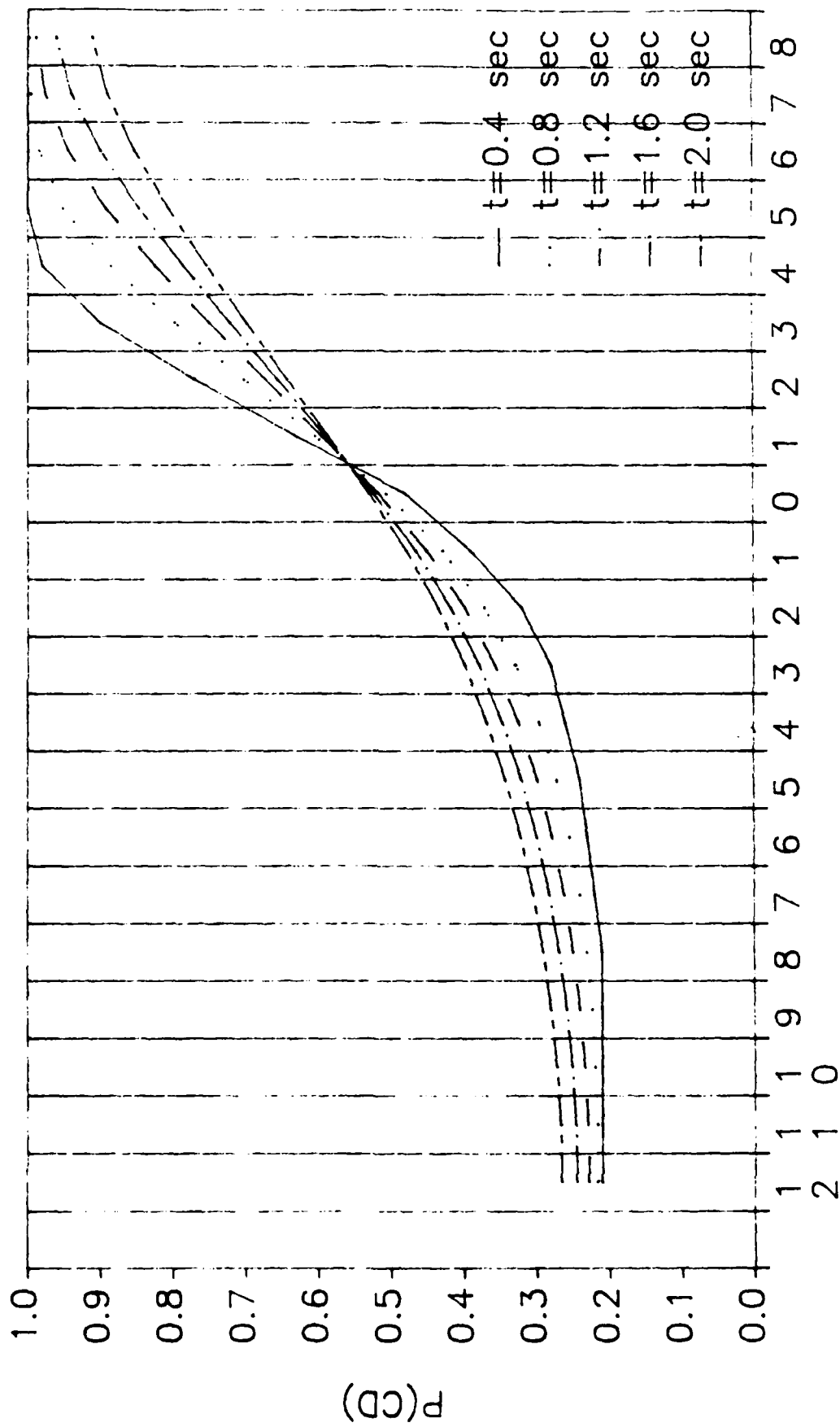
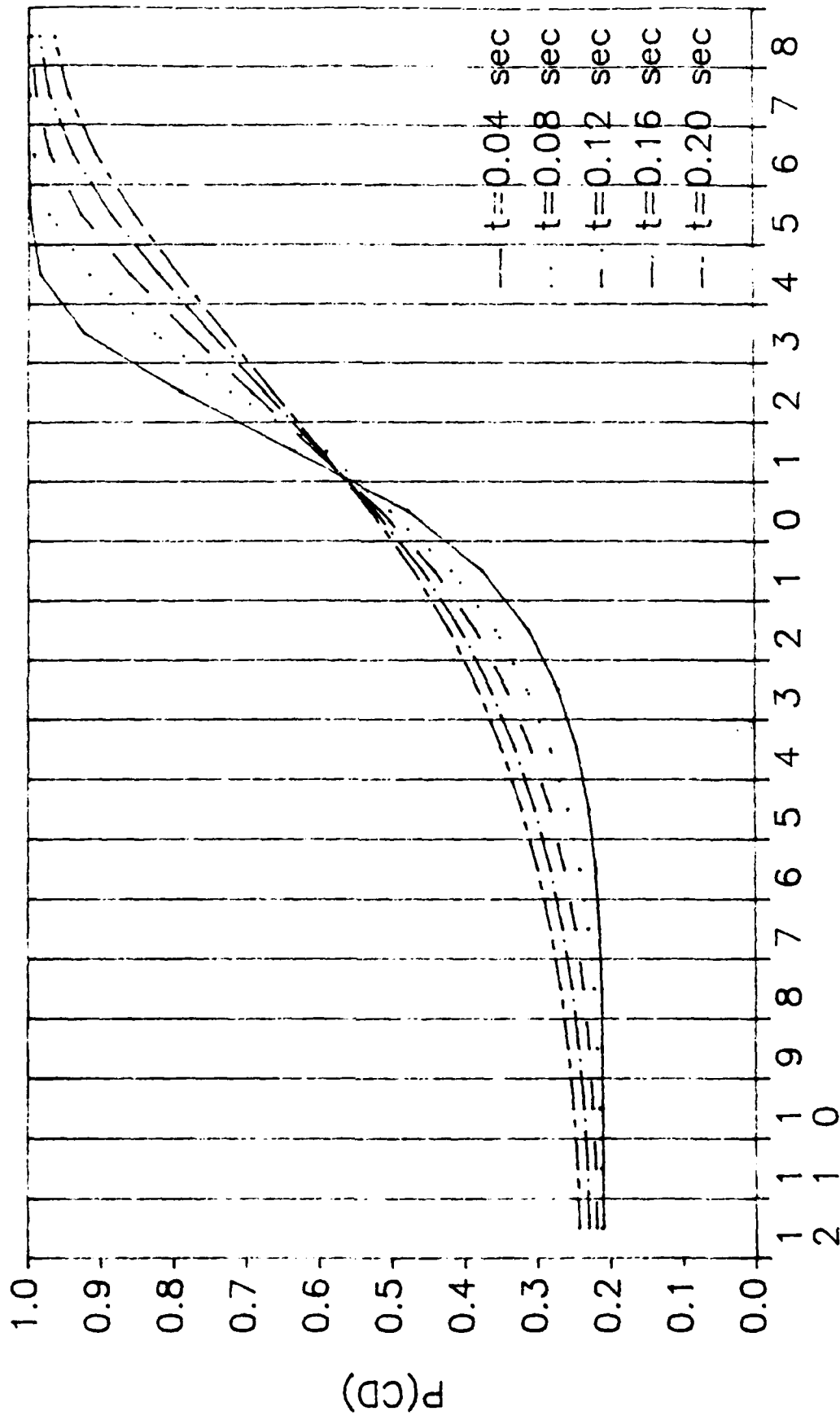


Fig 6(b). P(Cd) Profile at the Boundary
of Hg-Cd-Te/Cd-Te at 500 C.



Position of the Lattice Plane

Fig 6(c). P(Cd) Profile at the Boundary
of Hg-Cd-Te/Cd-Te at 550 C.



Position of the Lattice Plane

Fig 7(a). P(Cd) at the Lattice Plane 2m
vs. Time at 400 C.

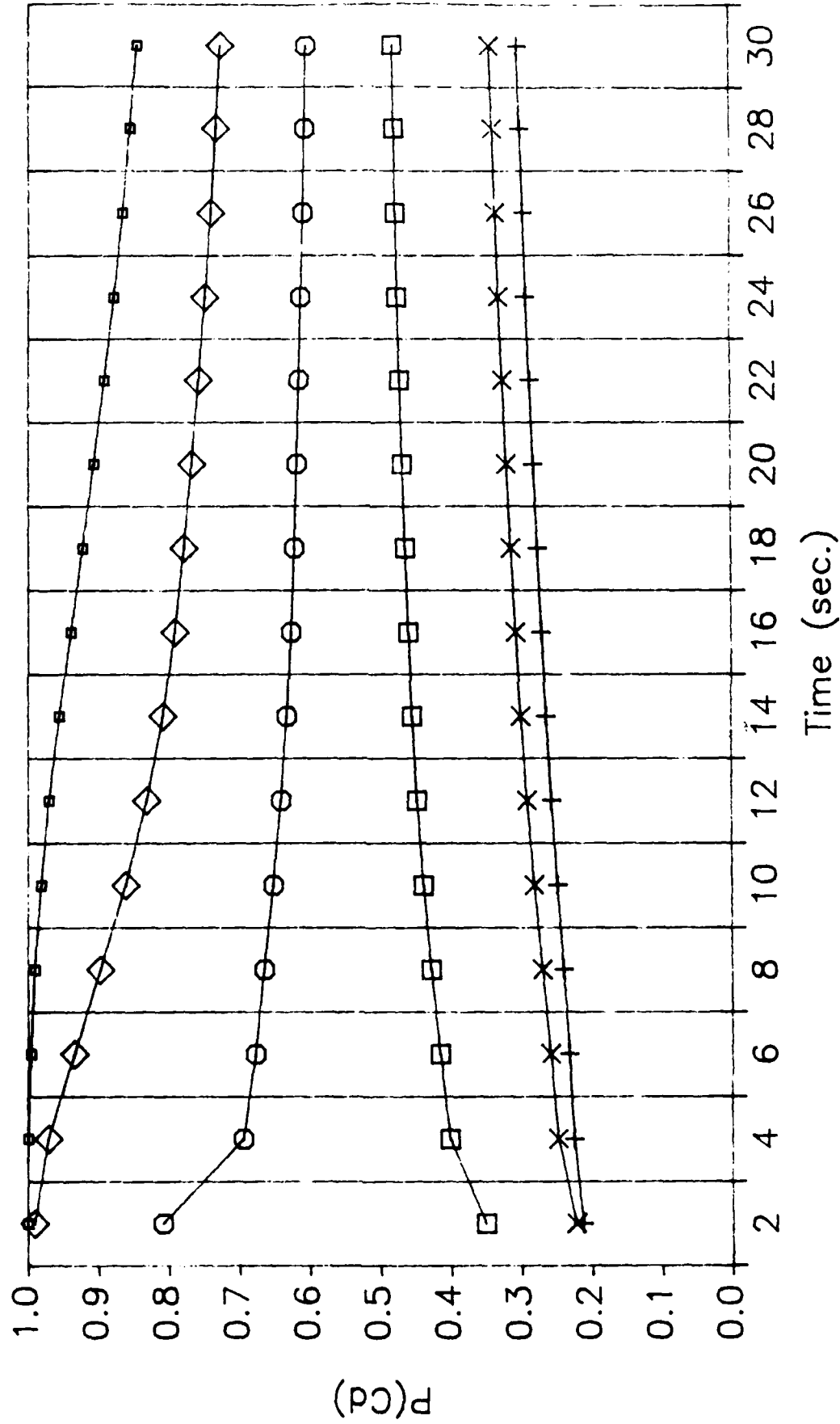
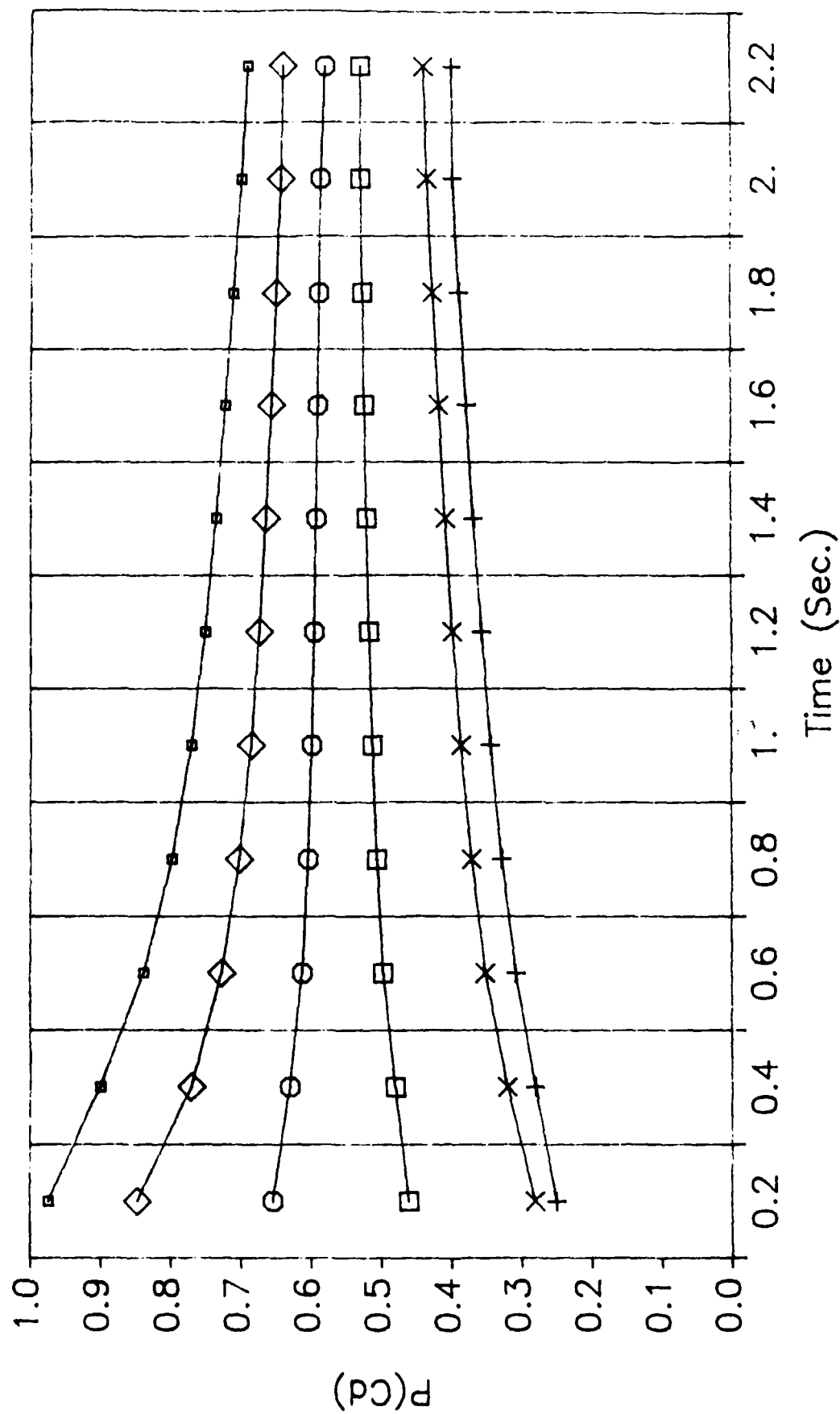
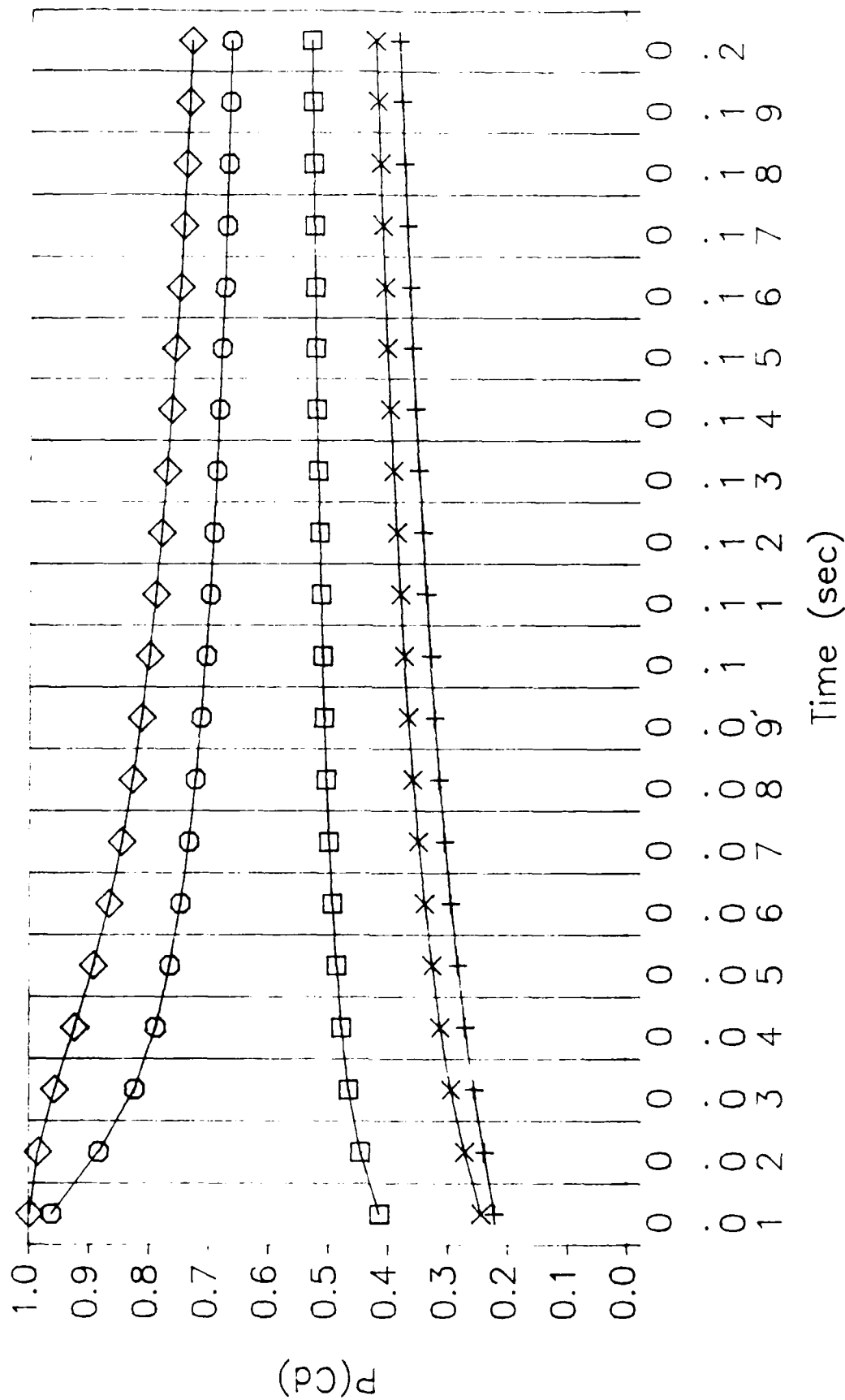


Fig 7(b). $P(\text{Cd})$ at the Lattice Plane $2m$
vs. Time at 500 C.



+ $m = -3$ x $m = -2$ □ $m = -1$ ◇ $m = 0$ ○ $m = 1$ ◇ $m = 2$ □ $m = 3$

Fig 7(c). $P(\text{Cd})$ at the Lattice Plane 2m
vs. Time at 550 C.



+ $m = -3$ \times $m = -2$ \square $m = 0$ \circ $m = 2$ \diamond $m = 3$

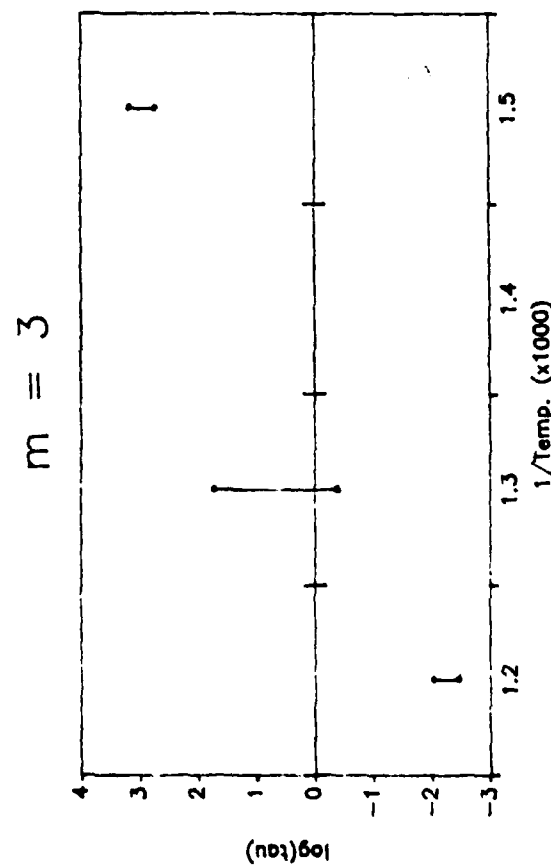
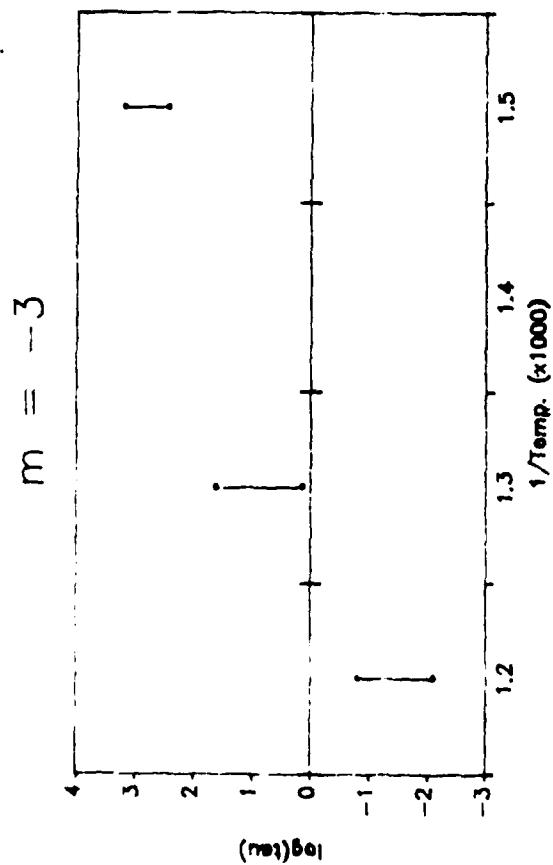
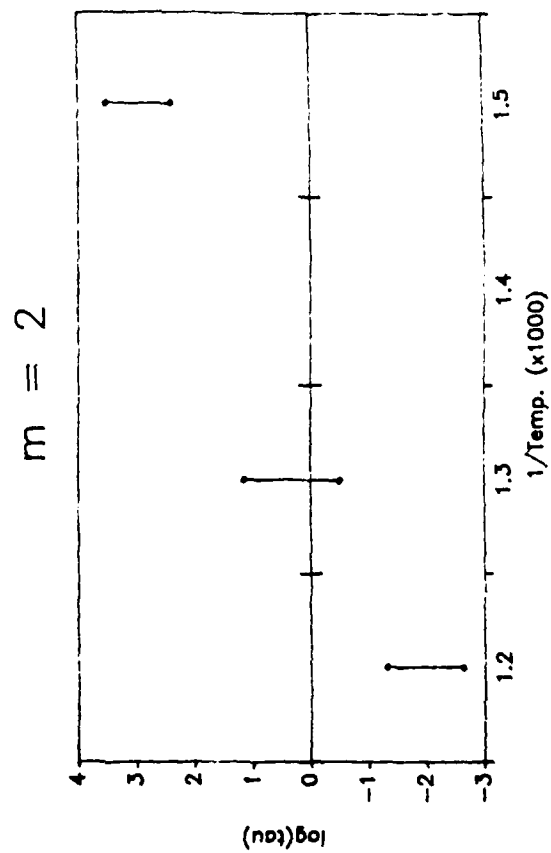
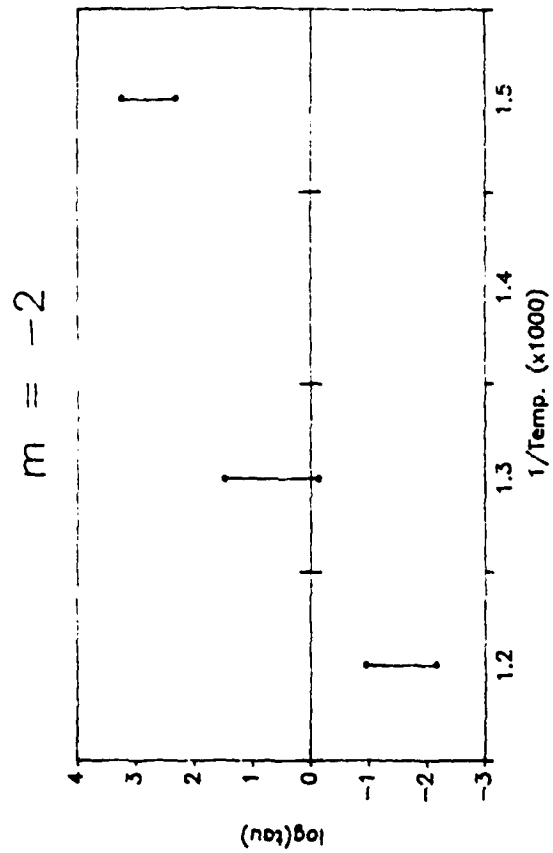
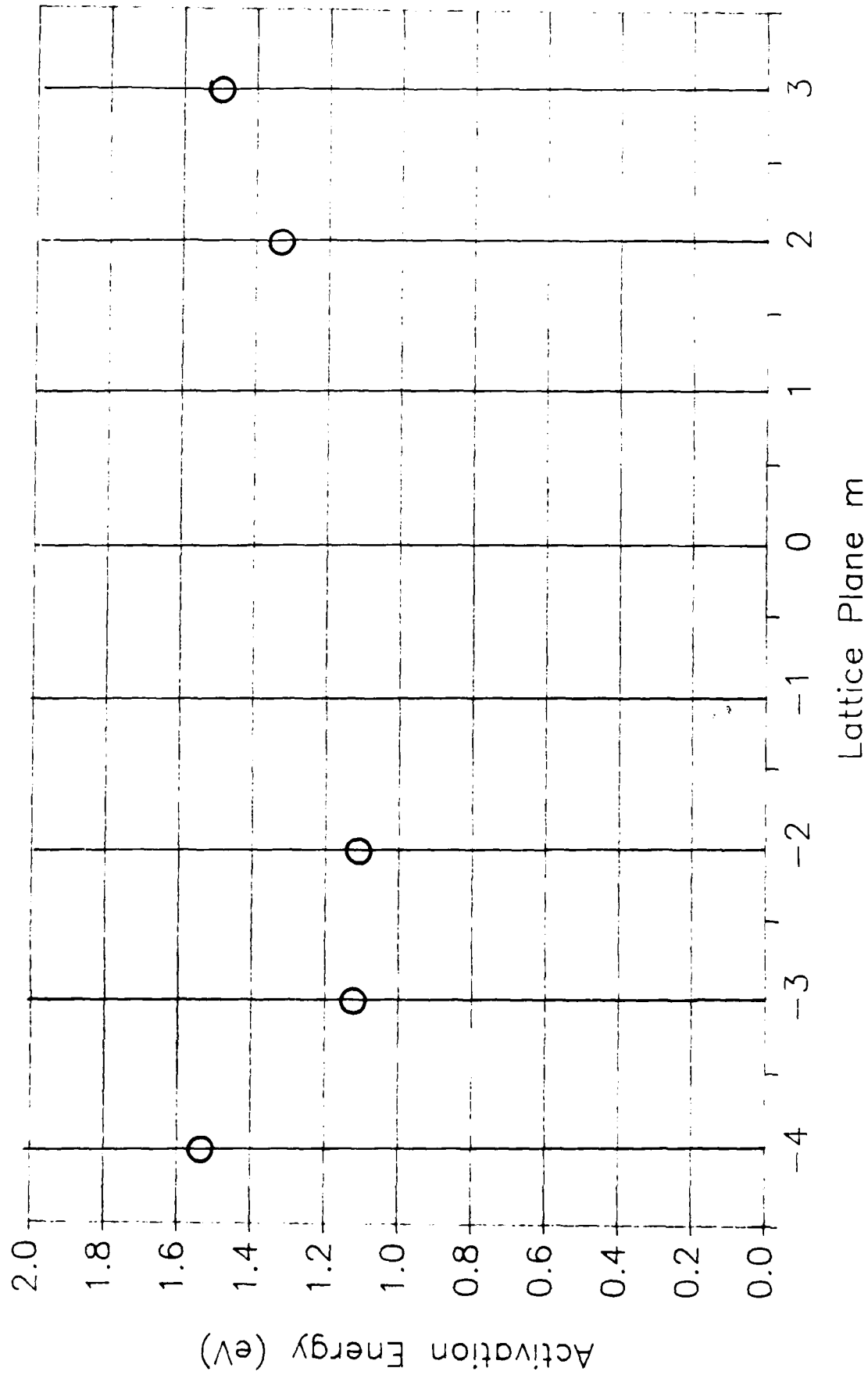


Figure 8. Relaxation times (τ) calculated from Figure 7 for different lattice plane positions.

Fig 9. Activation Energies for Lattice
Plane Positions



5. Summary and Conclusion

In semiconductor physics, study of kinetics of atomic migration is of great value in divergent applications. It will help understand crystal growth, material preparations, phase stability, radiation damage, and others. The present project is the first application of the path probability method (PPM) in this field. What we have done in the current contract period is naturally limited, but demonstrates possibility of future developments.

Main accomplishments are the following.

(1) The Hg and Cd diffusion in HgCdTe was formulated in terms of unit atomic jump mechanisms. Note that the PPM technique derives Fick's law from the microscopic atomic jump information.

(2) Based on his experiments on Hg vapor pressure (P_{Hg}) dependence of diffusion, Chen concluded that the fast diffusion of Hg is made of the vacancy mechanism branch and the interstitial mechanism branch. We confirmed this identification in our formulation.

(3) For the slow component of Hg diffusion, however, our interpretation is different from Chen's and is close to that of Tang and Stevenson⁶. We propose the $I \rightarrow III \rightarrow I$ jump mechanism for the slow diffusion, where I is the Hg-Cd sublattice and III is the interstitial sublattice (octahedral interstitial site with respect to the I sublattice). This diffusion mode is independent of P_{Hg} .

(4) We propose the similar $I \rightarrow III \rightarrow I$ mechanism for Cd diffusion. We cannot distinguish the slow and fast components, which were distinguished by Cheng.

(5) We used the Hg and Cd migration mechanism to calculate relaxation of the CdTe-HgCdTe junction. The rate controlling mechanism is the Cd migration which is slower than Hg. The relaxation of the boundary was computed.

(6) Based on the mechanism of (5), we estimated the relaxation time for the boundary relaxation is 1.6 hrs, 40 days and 2000 yrs for 300°C, 200°C and 100°C, respectively.

Thus the technique of irreversible statistical mechanics (PPM) used in formulating diffusion from atomic jump mechanism works well and leads to useful information. However, the technique needs improvements in several respects.

(A) The approximation of the project used the point as the basic cluster. It is desirable to use pairs to obtain more accurate results.

(B) The ionic nature of migrating species is to be taken into account more carefully.

(C) The method is promising in yielding useful information for studying diffusion and migration in many other compound semiconductors.

References

1. R. Kikuchi, "Theoretical calculation of Hg-Cd-Te liquidus-solidus phase diagram," J. Vac. Sci. Techn. Vol. 21 (1982) 129.
2. R. Kikuchi, "A theory of cooperative phenomena," Phys. Rev. Vol. 81 (1951) 988.
3. R. Kikuchi, "The path probability method," Prog. Th. Phys. (Kyoto) Suppl. No.35 (1966) p.1.
4. T. Ishikawa, W. Zhu and H. Sato, private communication.
5. J.-S. Chen, "Defect studies on crystalline solids", Ph.D. Thesis, University of Southern California, Jan. 1985.
6. M. S. Tang and D. A. Stevenson, Workshop on the Physics and Chemistry of HgCdTe (New Orleans) October 1987.

Figure Captions

- Figure 1(a)** The zincblende structure of the Hg-Cd-Te crystal. It is made of two fcc sublattices, I (white sphere) and II (black sphere).
- Figure 1(b)** Geometry of the I sublattice and the interstitial III sites.
- Figure 2** Relations between two main sublattices (I and III), and two interstitial sublattices (III and IV).
- Figure 3** The [111] projection of I and III sublattices, and the direction of the chemical potential gradient.
- Figure 4** (a) to (d) Experimental data of Hg and Cd diffusion after J. Chen⁵.
- Figure 5** Theoretical results of Hg diffusion (fast component) derived by the present work.
- Figure 6(a)** P(Cd) profile at the boundary of Hg-Cd-Te/Cd-Te at 400°C.
- Figure 6(b)** P(Cd) profile at the boundary of Hg-Cd-Te/Cd-Te at 500°C.
- Figure 6(c)** P(Cd) profile at the boundary of Hg-Cd-Te/Cd-Te at 550°C.
- Figure 7(a)** P(Cd) at the lattice plane 2m versus time at 400°C.
- Figure 7(b)** P(Cd) at the lattice plane 2m versus time at 500°C.
- Figure 7(c)** P(Cd) at the lattice plane 2m versus time at 550°C.
- Figure 8** Relaxation times (τ) calculated from Figure 7 for different lattice plane positions.
- Figure 9** Activation energies for lattice plane positions

END

DATE

FILMED

DTIC

JULY 88